ISSN 1318-0010
KZLTET 32(6)493(1998)

DECARBURIZATION MECHANISM OF Fe-Si-Al ALLOY WITH ANTIMONY ADDITION

MEHANIZEM RAZOGLJIČENJA ZLITINE Fe-Si-Al, LEGIRANE Z ANTIMONOM

DARJA STEINER PETROVIČ[1], M. JENKO[1], V. GONTAREV[2], H. J. GRABKE[3]

[1]Institute of Metals and Technology, Ljubljana, Slovenia
[2]University of Ljubljana, NTF-OMM, Ljubljana, Slovenia
[3]Max-Planck-Institut für Eisenforschung, Düsseldorf, Germany

Prejem rokopisa - received: 1998-12-06; sprejem za objavo - accepted for publication: 1998-12-14

The mechanism of decarburization process of Fe-Si-Al alloy was investigated on samples of cold rolled sheets; some of them alloyed with 0.048 wt.% Sb. The decarburization was performed in a H_2-H_2O gas mixture at 840°C. It was influenced by the oxidation of the surface. Antimony influence on decarburization mechanism of Fe-Si-Al alloy depends on carbon content in the steel.

Key words: decarburization, silicon steels, surface oxidation, antimony

Raziskali smo proces razogljičenja vzorcev Fe-Si-Al zlitin v obliki hladno valjane pločevine, ki smo jo legirali z 0.048 mas.% Sb. Razogljičenje je potekalo v atmosferi vlažnega vodika pri temperaturi 840°C. Na kinetiko razogljičenja vpliva tudi oksidacija površine jekla. Vpliv antimona na mehanizem razogljičenja zlitine Fe-Si-Al je bil povezan s koncentracijo ogljika v jeklu.

Ključne besede: razogljičenje, silicijeva jekla, oksidacija, oksidna plast, antimon

1 INTRODUCTION

The decarburization of Fe-Si-Al alloy - silicon steel is performed by annealing in a gas mixture of hydrogen and water vapour H_2-H_2O in the temperature range from 700 to 900°C with a controlled partial pressure ratio of water vapour and hydrogen $p(H_2O)/p(H_2)$. The decarburization process of steel in a gas mixture H_2-H_2O can be described by[1]:

1. Diffusion of carbon to the steel surface
2. Transport of water vapour to the steel surface and equilibration at the phase boundary steel-gas mixture
3. Dissociation of water vapour molecules into a hydrogen and oxygen and adsorption on the steel surface
4. Oxidation of carbon
5. Oxidation of iron and alloying elements

The major chemical reactions of decarburization of steel are:

$$[C]_{Fe} + O_{2(g)} = CO_{2(g)} \quad (1)$$

$$[C]_{Fe} + CO_{2(g)} = 2\ CO_{(g)} \quad (2)$$

$$[C]_{Fe} + 2\ H_{2(g)} = CH_{4(g)} \quad (3)$$

$$[C]_{Fe} + H_2O_{(g)} = CO_{(g)} + H_{2(g)} \quad (4)$$

$$[C]_{Fe} + 2\ H_2O_{(g)} = CO_{2(g)} + 2\ H_{2(g)} \quad (5)$$

The decarburization in a gas mixture of H_2-H_2O from 700 to 900°C proceeds predominantly according to reaction $[C]_{Fe} + H_2O_{(g)} = CO_{(g)} + H_{2(g)}$, the reaction according to $[C]_{Fe} + 2\ H_{2(g)} = CH_{4(g)}$ can be neglected at $p(H_2O)/p(H_2)$ greater than 0.01[2].

While the carbon is oxidised to gases CO and CO_2, the steel surface is continually oxidised to an oxide layer, which is influenced by alloying elements, affecting the scaling process of iron. When the alloying elements are less noble than iron then the possibility of internal oxidation arises, an external oxide layer may also be formed under circumstances which are normally protective to iron[3]. The following reactions of oxidation occur at the surface of the steel:

$$2\ Fe_{(s)} + O_{2(g)} = 2\ FeO_{(s)} \quad (6)$$

$$3\ Fe_{(s)} + 2\ O_{2(g)} = Fe_3O_{4(s)} \quad (7)$$

$$2\ Fe_{(s)} + 3/2\ O_{2(g)} = Fe_2O_{3(s)} \quad (8)$$

$$Fe_{(s)} + CO_{2(g)} = FeO_{(s)} + CO_{(g)} \quad (9)$$

$$Si_{(s)} + O_{2(g)} = SiO_{2(s)} \quad (10)$$

$$2\ Al_{(s)} + 3/2\ O_{2(g)} = Al_2O_{3(s)} \quad (11)$$

$$Mn_{(s)} + 1/2\ O_{2(g)} = MnO_{(s)} \quad (12)$$

2 EXPERIMENTAL

The samples were laboratory manufactured Fe-Si-Al alloys, hot and cold rolled strips with a final thickness of 1.5 mm and composition shown in **Table 1**. For thermogravimetric measurements samples were cut to a final dimension of 20 x 10 x 1,5 [mm^3], ground and polished with 1 μm grade diamond paste. All samples were cleaned in an ultrasound acetone bath.

The samples were submitted to decarburization annealing at 840°C in a gas mixture of hydrogen and water vapour with ratio $p(H_2O)/p(H_2)$ of 0.03 to 0.3. After decarburization the specimens were investigated by optical microscopy, SEM, and AES.

Table 1: Chemical composition of Fe-Si-Al alloys (wt.%)
Tabela 1: Kemična sestava zlitin Fe-Si-Al (mas.%)

Alloy No.	%C	%Si	%Al	%Mn	%P	%S	%Sb
2	0.260	1.74	1.19	0.23	0.0015	0.0023	-
3	0.009	1.40	0.70	0.25	0.0015	0.0020	0.048
4	0.010	1.55	0.70	0.25	0.0015	0.0024	-
6	0.280	1.94	0.80	0.17	0.0015	0.0023	0.048

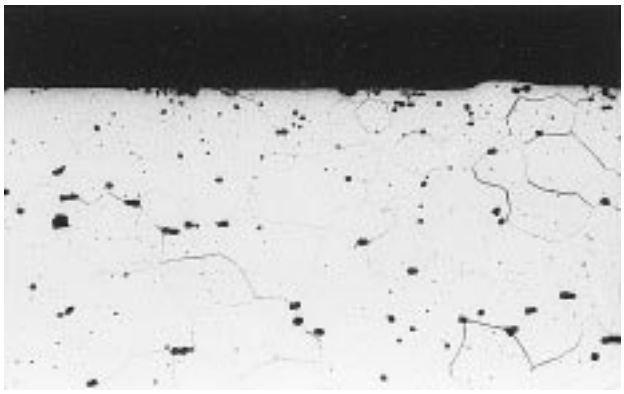

Figure 1: Ferrite microstructure of alloy No.2 after decarburization ($p(H_2O)/p(H_2)$=0.03, t=15 min, T=840°C, M 500x, Nital)
Slika 1: Feritna mikrostruktura zlitine No.2 po žarjenju za razogljičenje ($p(H_2O)/p(H_2)$=0.03, t=15 min, T=840°C, P 500x, Nital)

3 RESULTS AND DISCUSSION

Metallografic examination of annealed samples of Fe-Si-Al alloys showed that the decarburization process of Fe-Si-Al alloys at 840°C was efficient with exception of the alloy No.6 containing 0.28 wt.% C and 0.048 wt.% Sb. The microstructure of all decarburized steels after heat treatment consisted of polyhedral ferrite grains **(Figures 1,3,4)**. The grain growth of recrystallized grains depends on carbon content in the steel No.4,5. The grain growth rate was greater in decarburized steels and a coarse average grain size was obtained after decarburization. Decarburization in alloy No.6 took place only in a shallow layer under the surface **(Figure 2)**, where a ferritic microstructure with internal oxidation along the grain boundaries was formed. The microstructure of the non-decarburized part of the sample No.6 with 0.28 wt.%C and 0.048 wt.% Sb remained ferrite-pearlite.

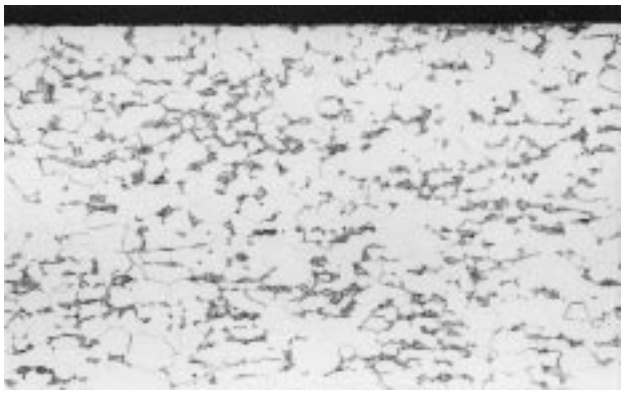

Figure 2: Ferrite-pearlite microstructure of alloy No.6 (with 0.048 wt.% Sb) after decarburization ($p(H_2O)/p(H_2)$=0.03, t=15 min, T=840°C, M 500x, Nital)
Slika 2: Feritno-perlitna mikrostruktura zlitine No.6 (z 0.048 mas.% Sb) po žarjenju za razogljičenje ($p(H_2O)/p(H_2)$=0.03, t=15 min, T=840°C, P 500x, Nital)

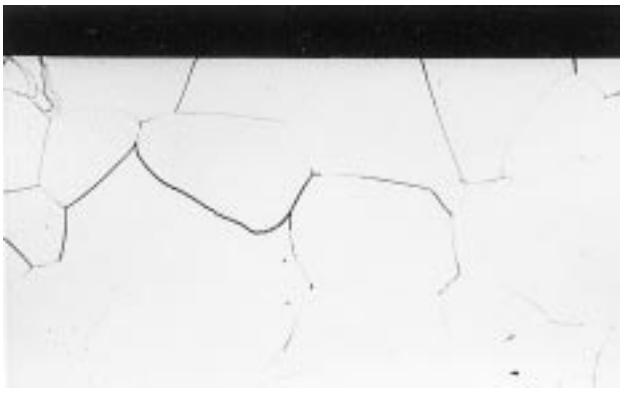

Figure 3: Ferrite microstructure of alloy No.3 (with 0.048 wt.% Sb) after decarburization ($p(H_2O)/p(H_2)$=0.03, t=15 min, T=840°C, M 500x, Nital)
Slika 3: Feritna mikrostruktura zlitine No.3 (z 0.048 mas.% Sb) po žarjenju za razogljičenje ($p(H_2O)/p(H_2)$=0.03, t=15 min, T=840°C, P 500x, Nital)

The samples of investigated steels were found to oxidise initially in a decarburizing atmosphere. The layers formed on the surface consisted of iron, aluminium and manganese oxides. The thickness of the oxide layer increased with increasing the time of annealing and the oxygen partial pressure in the gas mixture ($p(H_2O)/p(H_2)$). The surface oxidation during the decarburization was function of the temperature and oxygen potential and it was predominantly influenced by the behaviour of alloying elements Al and Mn.

Antimony was found to promote pearlite formation[6], therefore, the phase equilibrium in ferritic steel with an-

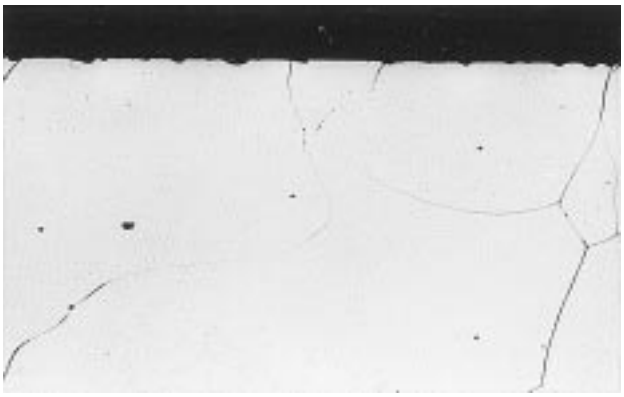

Figure 4: Ferrite microstructure of alloy No.4 after decarburization ($p(H_2O)/p(H_2)$=0.03, t=15 min, T=840°C, M 500x, Nital)
Slika 4: Feritna mikrostruktura zlitine No.4 po žarjenju za razogljičenje ($p(H_2O)/p(H_2)$=0.03, t=15 min, T=840°C, P 500x, Nital)

$$H_2O_{(g)} \rightarrow H_{2(g)} + 1/2O_{2(g)}$$
$$2\,H_2O_{(g)} \rightarrow 2\,H_{2(g)} + O_{2(g)}$$

$$1/2\,O_{2(ads)} + C_{(s)} \rightarrow CO_{(g)}$$
$$O_{2(ads)} + C_{(s)} \rightarrow CO_{2(g)}$$
$$CO_{2(g)} + C_{(s)} \rightarrow 2\,CO_{(g)}$$
$$3/2\,O_{2(ads)} + 2\,Al_{(s)} \rightarrow Al_2O_{3(s)}$$
$$O_{2(ads)} + Si_{(s)} \rightarrow SiO_{2(s)}$$
$$1/2\,O_{2(ads)} + Fe_{(s)} \rightarrow FeO_{(s)}$$
$$1/2\,O_{2(ads)} + Fe_{(s)} \rightarrow FeO_{(s)}$$
$$1/2\,O_{2(ads)} + 3FeO_{(s)} \rightarrow Fe_3O_{4(s)}$$
$$O_{2(ads)} \rightarrow [O]_{Fe}$$
$$3\,[O]_{Fe} + 2[Al]_{Fe} \rightarrow Al_2O_{3(s)}$$
$$2[O]_{Fe} + [Si]_{Fe} \rightarrow SiO_{2(s)}$$

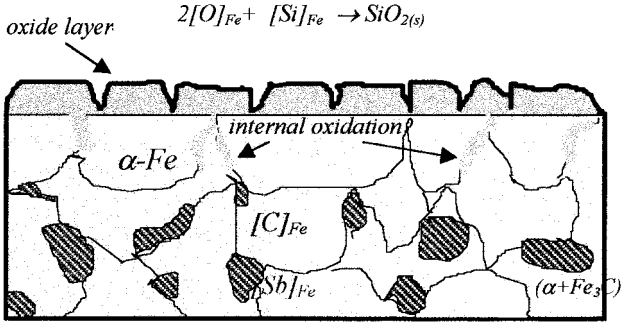

Figure 5: Mechanism of decarburization of Fe-Si-Al alloy with 0.28 wt.% C and 0.048 wt.% Sb
Slika 5: Mehanizem razogljičenja zlitine Fe-Si-Al z 0.28 mas.% C in 0.048 mas.% Sb

timony addition is established by more precipitated and less carbon in solid solution[7]. The smaller rate of decarburization of steel with antimony addition supports this hypothesis. Since the oxidation of carbon in Fe-Si-Al alloy with 0.28 wt.% C and 0.048 wt.% Sb was rather slow, the oxide layer formed on the surface of alloy No.6 was very compact. The surface and the internal oxidation during the decarburization of antimony doped Fe-Si-Al alloy has already been discussed in reference[8]. The continuous formation of gas molecules of CO and CO_2 during the decarburization of alloy No.2 resulted in a blis-

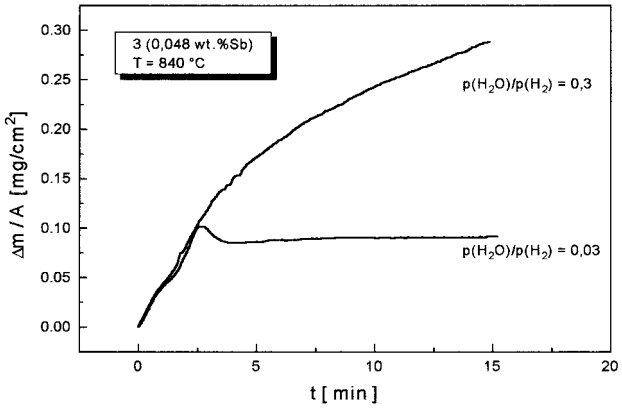

Figure 6: Kinetics of oxidation of Fe-Si-Al alloy with 0.009 wt.% C and 0.048 wt.% Sb during heat treatment at 840°C
Slika 6: Kinetika oksidacije zlitine Fe-Si-Al z 0.009 mas.% C in 0.048 wt.% Sb med žarjenjem pri 840°C

$$H_2O_{(g)} \rightarrow H_{2(g)} + 1/2O_{2(g)}$$
$$2\,H_2O_{(g)} \rightarrow 2\,H_{2(g)} + O_{2(g)}$$
$$1/2\,O_{2(ads)} + C_{(s)} \rightarrow CO_{(g)}$$
$$O_{2(ads)} + C_{(s)} \rightarrow CO_{2(g)}$$
$$[Sb]_{Fe} \rightarrow Sb_{segr}$$
$$2\,Sb_{(l)} + 3\,H_{2\,(g)} \rightarrow 2\,SbH_{3(g)}$$

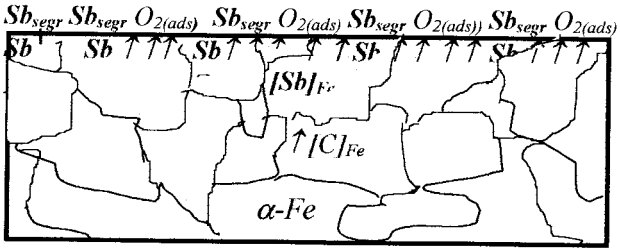

Figure 7: Mechanism of decarburization of Fe-Si-Al alloy with 0.009 wt.% C and 0.048 wt.% Sb
Slika 7: Mehanizem razogljičenja zlitine Fe-Si-Al z 0.009 mas.% C in 0.048 mas.% Sb

ters and cracks in the oxide scale[8]. The transport of carbon oxides can occur only through cracks and pores because the solubility and diffusivity of carbon in oxides and oxide scales are extremely small[9].

On the thermogravimetric curve of Fe-Si-Al alloy No.3 containing 0.009 wt.% C and 0.048 wt.% Sb the mass loss due to decarburization at $p(H_2O)/p(H_2) = 0.03$ was more pronounced than the mass gain due to oxidation **(Figure 6)**.

The less oxidised surface of Fe-Si-Al alloy No.3 after decarburization is likely to be the result of antimony surface segregation. Due to a low carbon content in the steel, the surface segregation of antimony[10-17] hindered the dissociation reaction of water vapour molecules and the oxidation of the steel surface as well[18] **(Figure 7)**.

4 SUMMARY

The decarburization mechanism of Fe-Si-Al alloys in a H_2-H_2O gas mixture at 840°C depends on the diffusion of carbon to the steel surface and chemical reactions on the surface.

During the decarburization of steel sheets in a flow apparatus mass gain was observed which implies on the oxidation of the steel surface. The oxidation of carbon on the steel surface was a function of temperature, oxygen potential of the atmosphere and was influenced by the selective oxidation of alloying elements Si, Al and Mn which have a higher affinity toward oxygen than iron. The thickness of the oxide layers increased with increasing time of decarburization annealing. The formation of oxide layers was a function of temperature and oxygen potential of the atmosphere as well. Formation of gaseous molecules due to high decarburization ability of antimony free alloy with 0.26 wt.% C resulted in porous and cracked oxide layer.

The influence of antimony on the decarburization mechanism of Fe-Si-Al alloys is associated with carbon content in the steel.

Antimony addition in Fe-Si-Al alloy decreases the solubility of carbon, promotes precipitation of carbides and delays decarburization process. The decarburization process of Fe-Si-Al alloy containing 0.28 wt.% C and 0.048 wt.% Sb was hindered by a protective oxide layer and the steel could be decarburized only beneath the surface. The oxide layer was more compact in comparison to antimony free alloys. Internal oxidation along grain boundaries affected the course of oxidation in the Fe-Si-Al alloys containing 0.048 wt.% Sb.

On the other hand, the decarburization process of Fe-Si-Al alloy containing 0.009 wt.% C and 0.048 wt.% Sb at $p(H_2O)/p(H_2) = 0.03$ was more efficient due to a surface segregation of antimony. Antimony segregating to the steel surface hindered the dissociation reaction of water vapour molecules and oxidation of the steel surface.

ACKNOWLEDGEMENT

The investigation was supported by Ministry of Science and Technology, Slovenia through the project J2-7228-206 and Max-Planck-Gesellschaft, Germany.

5 REFERENCES

[1] L. L. Shreir, R. A. Jarman, G. T. Burstein, *Corrosion*, Vol.1, Metal/Environment Reactions, Third Edition, Butterworth-Heinemann, Oxford, 1995

[2] H. J. Grabke, G. Tauber, *Arch. Eisenhüttenwes.*, 46 (1975) 3, 215-222

[3] N. Birks, in *Decarburization*, The Iron and Steel Institute, London, 1970, 1-11

[4] D. Steiner, M. Jenko, F. Vodopivec, *Kovine, zlitine, tehnologije*, 28 (1994) 1-2, 125-129

[5] D. Steiner Petrovič, M. Jenko, F. Vodopivec, *Journal de Physique IV*, 5 (1995) C7, 255-258

[6] E. N. Pan, C. Y. Chen, *American Foundry Men Society Transactions*, 70 (1996) 845-858

[7] F. Vodopivec, M. Jenko, D. Steiner Petrovič, B. Breskvar, F. Marinšek, *Steel Research*, 68 (1997) 80-86

[8] D. Steiner Petrovič, M. Jenko, F. Vodopivec, H. J. Grabke, *Kovine, zlitine, tehnologije*, 31 (1997) 3-4, 209-211

[9] P. Kofstad, A. Rahmel, R. A. Rapp, D. L. Douglass, *Oxidation of Metals*, 32 (1989) 1/2, 125-166

[10] H. J. Grabke, *ISIJ Int.*, 29 (1989) 529-533

[11] C. L. Briant, A. M. Ritter, *Acta Metall.*, 32 (1984) 2031-2042

[12] G. Lyudkovsky, P. K. Rastogi, M. Bala, *Journal of Metals*, 1 (1986) 18-25

[13] M. Rüsenberg, H. Viefhaus, *Surf. Sci.*, 172 (1986) 615-619

[14] M. Jenko, F. Vodopivec, B. Praček, M. Godec, D. Steiner, *J. Mag. Mat.*, 133 (1994) 229-232

[15] M. Jenko, F. Vodopivec, H. Viefhaus, M. Milun, T. Valla, M. Godec, D. Steiner Petrovič, *Fizika*, A4 (1995) 3, 91-98

[16] M. Jenko, F. Vodopivec, H. J. Grabke, H. Viefhaus, M. Godec, D. Steiner Petrovič, *Journal de Physique IV*, 5 (1995) C7, 225-231

[17] R. Mast, *PhD Thesis*, University of Dortmund, Germany, 1996

[18] D. Steiner Petrovič, *MD Thesis*, University of Ljubljana, Slovenia, 1998